J Fluoresc (2015) 25:529–539
DOI 10.1007/s10895-015-1522-4

ORIGINAL PAPER

Novel Multiporphyrin Functionalized Single-Walled Carbon Nanotubes

Gülsiye Öztürk Ürüt · Demet Karakaş · Chandan Maity

Received: 10 October 2014 / Accepted: 20 January 2015 / Published online: 25 March 2015
© Springer Science+Business Media New York 2015

Abstract Porphyrin monomers, 5,15–bis(4-(2,5,8,11-tetraoxatridecan-13-yloxy)phenyl)-10,20-bis(3-iodophenyl)porphyrin zinc (5a) and 5,10–bis(4-(2,5,8,11-tetraoxatridecan-13-yloxy)phenyl)-15,20-bis(3-iodophenyl)porphyrin zinc (5b), and their oligomers 6a and 6b were synthesized and characterized. The titration experiment of the monomers was carried out in THF by changing the solution percent of water. The optical properties (UV–vis and fluorescence spectra) of the monomers that possess slightly red-shifted optical spectra in water compared to the spectra obtained in THF are reported. The newly prepared porphyrin constructs were also mixed with SWCNTs to generate noncovalent hybrid materials.

Keywords Porphyrin · SWCNT · Multiporpyrin · Fluorescence

Introduction

Porphyrins are of major interest in chemistry and have thus been subjected to intensive experimental and theoretical investigations [1–46]. Porphyrins with tailor-made photophysical properties and well-defined three-dimensional geometries constitute attractive synthetic targets in porphyrin chemistry [1]. Porphyrins are a ubiquitous class of naturally occurring compounds within important biological representatives such as hemes, chlorophyll, and Vitamin B_{12} [2, 3]. They perform important chemical processes, such as (photoinduced) electron transfer, oxygen-binding and C-H bond activation [1, 3]. The basic structure of the Por macro cycle consists of four pyrrolic subunits linked by four methine bridges [2]. A great number of structural changes consisting of variation of the central atom and/or peripheral substituents at the unoccupied pyrrolic positions can be achieved without altering the porphyrin's chemical stability [2, 4]. Among the many promising examples are large excited state absorption cross-sections and various other nonlinear optical effects as well as long triplet excited state life times. These properties render porphyrins interesting candidates for generating effective optical limiting materials. Since the invention of intense light sources based on laser mechanism in 1960s, the need for protection of optical sensors and human eyes from accidental and hostile lasers has stimulated considerable research. More recently several materials (organic and organometallic compounds with nonlinear optical properties) and device configurations have been proposed and developed to meet this challenge, among these materials porphyrins are very attractive due to their intrinsic properties and the fact that they can be readily be tuned by suitable structural modifications.

During the last years, efforts have been made to encapsulate porphyrins within dendrimers to tune their photophysical, electrochemical and chemical properties [5–8]. Because of their large size and the possibility of host-guest interactions the porphyrins represent attractive cores for the design of dendritic sensors and catalysts [5]. Porphyrins and metalloporpyrins are also useful photophysical probes for evaluating properties of dendimeric structure due to their sensitivity to the type and position of the substitution as well as the presence of neighbouring chromophores.

G. Ö. Ürüt · C. Maity
Laboratory of Organic Chemistry and Functional Materials, Department of Chemistry, Humboldt University, Brook-Taylor-Str. 2, 12489, Berlin Adlershof, Germany

G. Ö. Ürüt (✉) · D. Karakaş
Department of Chemistry, Faculty of Sciences, Dokuz Eylül University, Tinaztepe Campus, 35160 Buca, Izmir, Turkey
e-mail: gulsiye.ozturk@deu.edu.tr

G. Ö. Ürüt
e-mail: gulsiyeozturk@yahoo.com

The success of the photosynthetic reaction centre as a transducer of light into chemical potential depends primarily on the assembly being able to exert strict control over a number of design features, such as the separation and orientation of the various redox centres and the nature of the medium separating those [9]. Therefore, an important aspect of designing artificial photosynthetic devices based particularly on the multiporphyrin arrays found in light harvesters and in the initial processes of such reaction centres, is the selection of an appropriate organizing principle that will control these same features. Multiporphyrin systems in which the porphyrin subunits are interlinked using covalent bonds have produced an array of elegant structures, some of which enable mimicking those processes found in natural reaction centres.

Nature's process of electron transport has been mimicked in the form of an electron donor/acceptor (D/A) pair utilizing porphyrin derivatives as electron donors combined with complementary electron-accepting species [14]. Among the many promising examples are large excited state absorption cross-sections and various other nonlinear optical effects as well as long triplet excited state life times. These properties render porphyrins interesting candidates for generating effective optical limiting materials. [14, 15]. It is also reported that fullerenes have been spontaneously attracted to porphyrins and metalloporphyrins [10, 14, 16–20]. A natural feature of these structures is the cofacial sandwich-like arrangement of porphyrins with fullerenes bound in the clefts.

Complex mixtures of nanometer-sized graphene cylinders are commonly referred to nowadays as single-walled carbon nanotubes (SWCNTs), have captured the imagination of scientists and engineers largely because of their remarkable physicochemical, mechanical, and electronic properties. Therefore they constitute exciting new materials for creating next generation optoelectronic devices, ranging from field-effect transistor devices, chemical sensors, molecular switch tunnel junctions and photovoltaic devices, integrated multifunctional sensors and devices, among others [14, 21–23, 25]. The insolubility of the SWNTs in most solvents and the difficulties of handling these highly intractable carbon nanostructures, however, are restricting their real-life applications at the present time [22, 23]. Thus to improve upon the properties of the SWNTs, low-cost and industrially feasible approaches to their modifications are constantly being sought by chemists and materials scientists. Among these approaches, noncovalent supramolecular modifications of the SWNTs can do much to preserve the desired properties of the SWNTs, while remarkably improving their solubilities. For example, it is reported that the noncovalent combination of the SWNTs with pyrene and porphyrin derivatives leads to novel electron donor-acceptor nanohybrids, which, upon photoexcitation, undergo fast electron-transfer, followed by the generation microsecond-lived charge-separated species [22, 24, 25]. Moreover, success in the noncovalent functionalization of the SWNTs has provided a further opportunity to employ these entitites as chemical and/or biological sensors.

In this work we synthesized novel porphyrin monomers, 5, 15–bis(4-(2,5,8,11-tetraoxatridecan-13-yloxy)phenyl)-10,20-bis(3-iodophenyl)porphyrin zinc (5a) and 5,10–bis(4-(2,5,8,11-tetraoxatridecan-13-yloxy)phenyl)-15,20-bis(3-iodophenyl)porphyrin zinc (5b), and their porphyrin oligomers 6a and 6b (Scheme 1). After their structural characterization, the newly prepared porphyrin constructs were mixed with SWCNTs to generate noncovalent hybrid materials. These were investigated with regard to their absorption and emission properties Scheme 1.

Experimental

Materials and Instrumentation

Solvents and starting materials were used as received. Pyrrole was freshly distilled before use. Tetrahydrofuran (THF), dichloromethane (DCM) and dimethylformamid (DMF) were distilled under an argon atmosphere over Na or CaH_2 prior to use. Reactions were monitored by thin layer chromatography (TLC) carried out on silica gel plates (Merck 60 F-254) using UV light for visualization. Silica gel (Merck 60, particle size 0.040–0.063 mm) was used for column chromatography. Microwave assisted poylcondensations were performed in a microwave reactor.

NMR spectra were recorded on Bruker AC500 (500 MHz) spectrometer using residual protonated solvent signals as the internal standard (^{1}H-NMR: δ (CDCl3)=7.26 ppm, and ^{13}C-NMR: δ (CDCl3)=77.16 ppm). GPC measurements in THF as the mobile phase were performed on a WGE Dr. Bures system equipped both with a Knauer UV 2500 and Knauer RI K-2301 detector at 60°C using a flow rate of 1 ml/min. The samples were separated through a series of four columns (SDV 50A 5u PPS, SDV 500A 5u PPS, SDV 100A 5u PL-Gel, SDV 5 μ Linear M PSS). Ultra performance liquid chromatography coupled to mass spectrometry detection (UPLC-MS) was performed with a Waters Alliance systems (gradient mixtures of acetonitrile/water) equipped with Acquity UPLC columns. The Waters systems consisted of a Waters Separations Module 2695, a Waters Diode Array detector 996, a LCT Premier XE mass spectrometer, and a Waters Mass Detector ZQ 2000.

Scheme 1 Synthesis of **6a-b**: *i*) TsCl, THF, tetraethyleneglycolmonomethylether, NaOH, H_2O , *ii*) 4-hydrohybenzaldehyde, DMF, K_2CO_3 , *iii*) pyrrole, TFA, *iv*) 3-iodobenzaldehyde, CH_2Cl_2 , $BF_3.O(Et)_2$, DDQ, *v*) $CHCl_3$, *vi*) TMSA, THF, diisopropylamine ▶

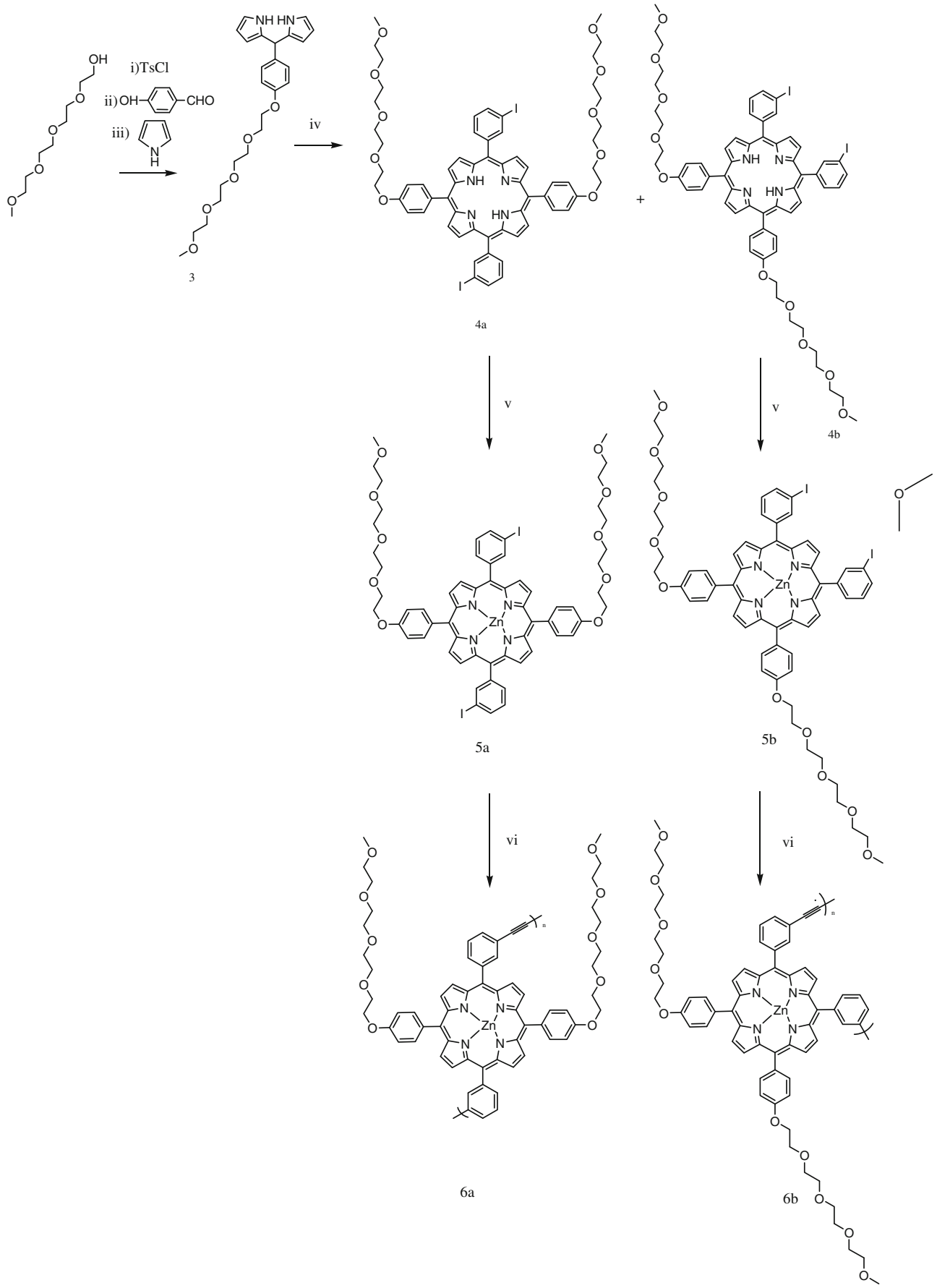
i)TsCl
ii)
iii)
iv
v
vi
3
4a
4b
5a
5b
6a
6b

Table 1 Absorption and fluorescence emission maxima (λ, nm) of 5a, 5b, 6a, 6b, 6a-SWCNT and 6b-SWCNT

Compound	Solvent	$\lambda_{max\ abs}$ (nm)	$\lambda_{max\ emis}^{1}$ (nm)	$\lambda_{max\ emis}^{2}$ (nm)
5a	THF	426	605	654
	H2O	436	609	659
5b	THF	426	604	654
	H_2O	435	606	656
5a-SWCNT	THF	426	604	653
5b-SWCNT	THF	426	604	653
6a	THF	426	604	653
6b	THF	426	615	652
6a-SWCNT	THF	426	604	653
6b-SWCNT	THF	426	615	652

The absorption spectra were measured using a Shimadzu UV-1601 spectrophotometer. Fluorescence measurements were recorded using a Varian-Cary Eclipse spectrofluorimeter.

Synthesis of 2,5,8,11-tetraoxatridecan-13-yl-4-methylbenzenesulfonate (1)

Was prepared according to the literature [47, 48].

Synthesis of 4-(2,5,8,11-tetraoxatridecan-13-yloxy)benzaldehyde (2)

Was prepared according to the literature [49].

Synthesis of 2,2′-((4-(2,5,8,11-tetraoxatridecan-13-yloxy)phenyl)methylene)bis(1H-pyrrole) (3)

Pyrrole (1.4 ml, 20 mmol) and 4-(2,5,8,11-tetraoxatridecan-13-yloxy)benzaldehyde (0.25 g, 1.6 mmol) were added to a dry round-bottomed flask and degassed with a stream of Ar for 5 min. TFA (6.2 μl, 0.16 mmol) was then added and the solution was stirred under Ar at room temperature for 30 min and then quenched with 0.1 M NaOH: Ethyl acetate was then added. The organic phase was washed with water and dried ($MgSO_4$), and the solvent removed under vacuum to afford light yellow oil. Column chromatography with 1:1 EA:PE gave 0.1 g of 2,2′-((4-(2,5,8,11-tetraoxatridecan-13-yloxy)phenyl)methylene)bis(1*H*-pyrrole). Yield=51 %; R_f (EA : PE=1 : 1)=0.52; ^{1}H-NMR (500 MHz, $CDCl_3$): δ (ppm) 7.99 (s, 2H), 7.02 (d, 2H, *J*= 3.5 Hz), 6.76 (d, 2H, *J*=4.5 Hz), 6.59–6.58 (m, 2H), 6.06–6.04 (m, 2H), 5.81–5.79 (m, 2H), 5.32 (s, 1H), 4.01 (t, 2H, *J*= 2.5 Hz), 3.75 (t, 2H, *J*=2.3 Hz), 3.63–3.62 (m, 2H), 3.5884–3.5291 (m, 8H), 3.46–3.44 (m, 2H), 3.65 (s, 3H); ^{13}C-NMR (500 MHz, $CDCl_3$): δ (ppm) 67.5, 69.7, 70.5, 70.6, 70.8, 71.9, 106.9, 108.3, 114.7, 117.1, 129.4, 132.9, 134.6157.7; UPLC TOF MS ES+ : m/z=429.1279, calcd. m/z=429.2389

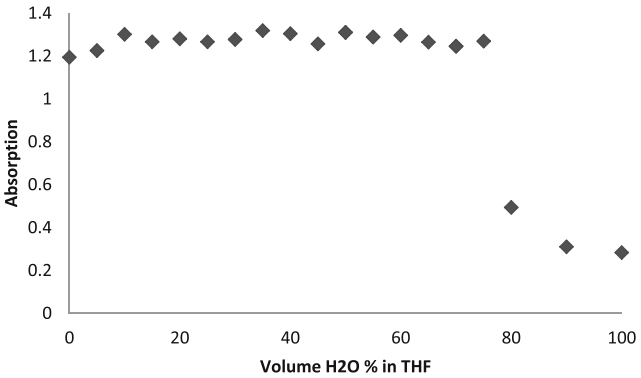

Fig. 2 Plot of absorption intensity of 10–6 M 5a vs the volume percent of water in THF. All the solutions prepared 5a content is 10–6 M

Synthesis of 5,15–bis(4-(2,5,8,11-tetraoxatridecan-13-yloxy)phenyl)-10,20-bis(3-iodophenyl)porphyrin (4a)

A solution of 3-iodobenzaldehyde (0.53 g, 2.3 mmol) and 2,2′-((4-(2,5,8,11-tetraoxatridecan-13-yloxy)phenyl)methylene)bis(1*H*-pyrrole) (1 g, 2.3 mmol) in CH_2Cl_2 (230 ml) was purged with N_2 and treated with $BF_3.O(Et)_2$ (87 μl, 0.69 mmol) at room temperature. After 3 h DDQ (0.8 g, 3.5 mmol) was added. Chromatography with EA:PE 1:1 and then EA gave 0.38 g of d1 and then

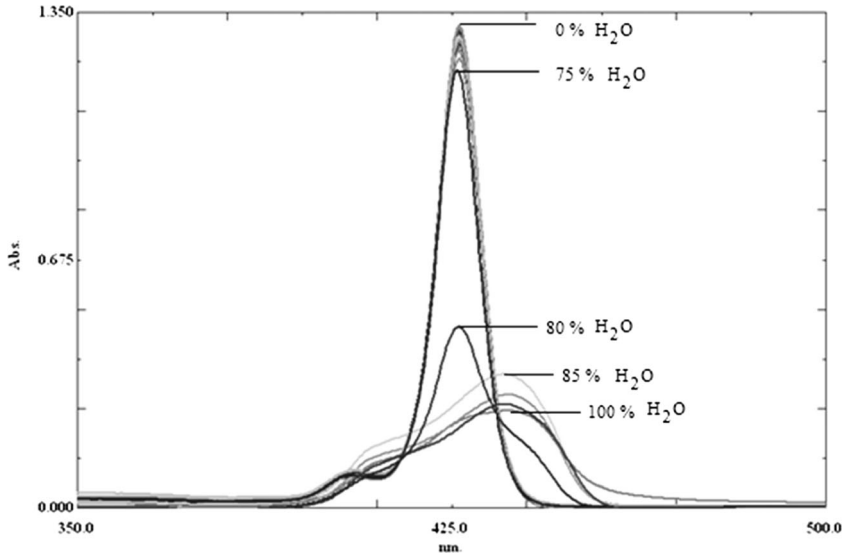

Fig. 1 Absorption spectra of titration experiment of 10–6 M 5a at different volume percent of water in THF. All the solutions prepared 5a content is 10–6 M

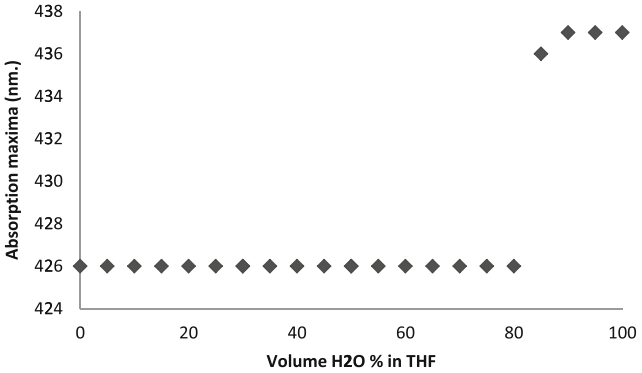

Fig. 3 Plot of absorption maxima of 10–6 M 5a vs the volume percent of water in THF. All the solutions prepared 5a content is 10–6 M

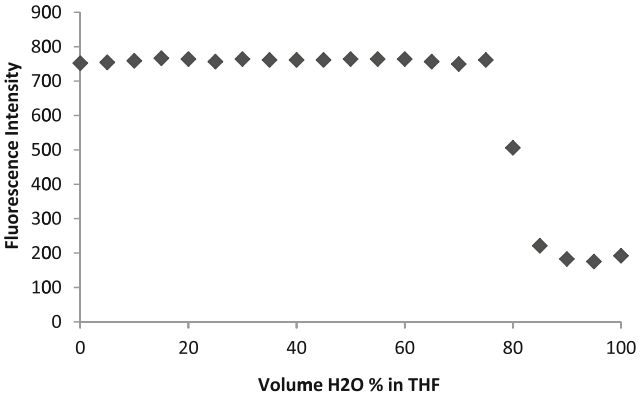

Fig. 5 Plot of fluorescence intensity of 10–6 M 5a vs the volume percent of water in THF. All the solutions prepared 5a content is 10–6 M

chromatography with EA:THF 1:1 gave 0.13 g of 5,10 – bis(4-(2,5,8,11-tetraoxatridecan-13-yloxy)phenyl)-15,20-bis(3-iodophenyl)porphyrin (d2) as a purple solid (yield= 13 % (4a) and 5 % (4b)). R_f (EA)=0.43 (d1) ; 0.18 (d2). ^{1}H-NMR (500 MHz, $CDCl_3$): δ (ppm) 8.83 (d, 4H, *J*=2.4 Hz), 8.76 (d, 4H, *J*=2.3 Hz), 8.46 (s, 2H), 8.10 (d, 2H, *J*=3.9 Hz), 8.07 (m, 2H), 8.03 (d, 4H, *J*=4.0 Hz), 7.41 (t, 2H, *J*=4.1 Hz), 7.23 (d, 4H, *J*=4.1 Hz), 4.35 (t, 4H, *J*=2.6 Hz), 3.98 (t, 4H, *J*= 2.6 Hz), 3.81–3.79 (m, 4H), 3.73–3.64 (m, 12H), 3.62–3.60 (m, 4H), 3.33 (s, 6H); UPLC TOF MS ES+ : $C_{62}H_{65}N_4O_{10}I_2$ m/z=1279.3094 , calcd. m/z=1279.2790; UV/vis (ACN): λ_{max}=417 nm.

Synthesis of 5,10–bis(4-(2,5,8,11-tetraoxatridecan-13-yloxy)phenyl)-15,20-bis(3-iodophenyl)porphyrin (4b)

A solution of 3-iodobenzaldehyde (0.53 g, 2.3 mmol) and 2,2′-((4-(2,5,8,11-tetraoxatridecan-13-yloxy)phenyl)methylene)bis(1*H*-pyrrole) (1 g, 2.3 mmol) in CH2Cl2 (230 ml) was purged with N2 and treated with $BF_3.O(Et)_2$ (87 μl, 0.69 mmol) at room temperature. After 3 h DDQ (0.8 g, 3.5 mmol) was added. Chromatography with EA:PE 1:1 and then EA gave 0.38 g of 4a and then chromatography with EA:THF 1:1 gave 0.13 g of 5,10 – bis(4-(2,5,8,11-tetraoxatridecan-13-yloxy)phenyl)-15,20-bis(3-iodophenyl)porphyrin (4b) as a purple solid (yield=13 % (4a) and 5 % (4b)). R_f (EA)=0.43 (d1) ; 0.18 (d2). ^{1}H-NMR (500 MHz, $CDCl_3$): δ (ppm) 8.81–8.79 (m, 4H), 8.75–8.74 (m, 4H), 8.50 (s, 2H), 8.09 (d, 2H, *J*=3.7 Hz), 8.04 (m, 2H), 8.02 (d, 4H, *J*=4.3 Hz), 7.39 (t, 2H, *J*=4.2 Hz), 7.21 (d, 4H, *J*=4.3 Hz), 4.33 (t, 4H, *J*=2.3 Hz), 3.96 (t, 4H, *J*=2.6 Hz), 3.79–3.77 (m, 4H), 3.77–3.63 (m, 12H), 3.61–3.59 (m, 4H), 3.50–3.49 (m, 4H), 3.31 (s, 6H); UPLC TOF MS ES+: $C_{62}H_{65}N_4O_{10}I_2$ m/z=1279.8253, calcd. m/z=1279.2790; UV/vis (ACN): λ_{max}=417 nm

Synthesis of 5,15–bis(4-(2,5,8,11-tetraoxatridecan-13-yloxy)phenyl)-10,20-bis(3-iodophenyl)porphyrin zinc (5a)

To a stirred solution of 5,15 – bis(4-(2,5,8,11-tetraoxatridecan-13-yloxy)phenyl)-10,20-bis(3-iodophenyl)porphyrin (160 mg, 12.5 μmol) in chloroform (13 ml) a solution of zinc acetate dihydrate (0.14 g,) in MeOH (1.4 ml) was added. The reaction was stirred for 1 h at 60°C.

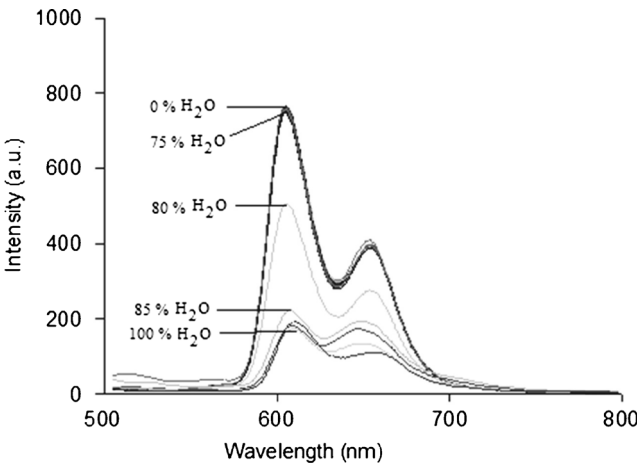

Fig. 4 Fluorescence spectra of titration experiment of 10–6 M 5a at different volume percent of water in THF using an excitation wavelength of 426 nm. All the solutions prepared 5a content is 10–6 M

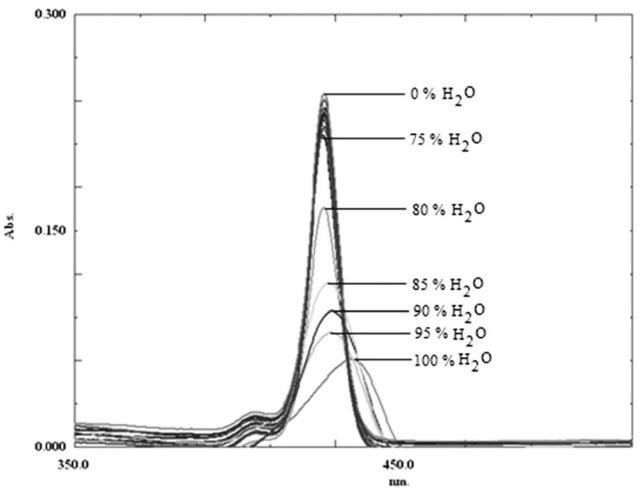

Fig. 6 Absorption spectra of titration experiment of 10–6 M 5b at different volume percent of water in THF. All the solutions prepared 5b content is 10–6 M

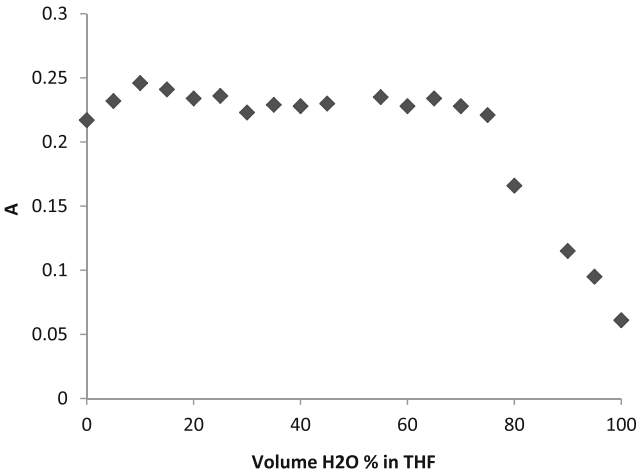

Fig. 7 Plot of absorption intensity of 10–6 M 5b vs the volume percent of water in THF. All the solutions prepared 5b content is 10–6 M

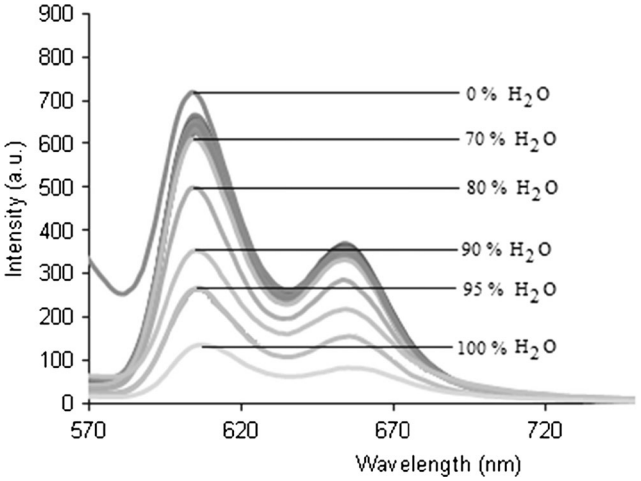

Fig. 9 Fluorescence spectra of titration experiment of 10–6 M 5b at different volume percent of water in THF using an excitation wavelength of 426 nm. All the solutions prepared 5b content is 10–6 M

Evaporation of the solvent and chromatography on silica, eluting with EA gave 100 mg of 5,15 – bis(4-(2,5,8,11-tetraoxatridecan-13-yloxy)phenyl)-10,20-bis(3-iodophenyl)porphyrin zinc (Yield=% 60). R_f (EA)=0.5; ^{1}H-NMR (500 MHz, $CDCl_3$): δ (ppm) 8.86 (d, 4H, *J*=2.4 Hz), 8.81(d, 4H, *J*=2.3 Hz), 8.49 (s, 2H), 8.11 (d, 2H, *J*=3.4 Hz), 8.02 (d, 2H, *J*=3.9 Hz), 7.97 (d, 4H, *J*=4.0 Hz), 7.41–7.37 (m, 2H), 7.03 (d, 4H, *J*=4.1 Hz), 3.99–3.97 (m, 4H), 3.62–3.59 (m, 4H), 3.38–3.37 (m, 4H), 3.32–3.31 (m, 4H), 3.28–3.27 (m, 4H), 3.22–3.20 (m, 4H), 3.11–3.09 (m, 4H), 2.97 (s, 6H); UPLC TOF MS ES+ : $C_{62}H_{63}N_4O_{10}ZnI_2$ m/z=1341.6819, calcd. m/z=1341.1925; UV/vis (ACN : THF): λ_{max}=424 nm.

Synthesis of 5,10–bis(4-(2,5,8,11-tetraoxatridecan-13-yloxy)phenyl)-15,20-bis(3-iodophenyl)porphyrin zinc (5b)

To a stirred solution of 5,10 – bis(4-(2,5,8,11-tetraoxatridecan-13-yloxy)phenyl)-15,20-bis(3-iodophenyl)porphyrin (170 mg, 12.7 μmol) in chloroform (14 ml) a solution of zinc acetate dihydrate (0.14 g,) in MeOH (1.4 ml) was added. The reaction was stirred for 1 h at 60°C. Evaporation of the solvent and chromatography on silica, eluting with EA:THF 1:1 gave 110 mg of 5,10 – bis(4-(2,5,8,11-tetraoxatridecan-13-yloxy)phenyl)-15,20-bis(3-iodophenyl)porphyrin zinc (Yield=61 %). R_f (EA:THF= 1:1)=0.83; ^{1}H-NMR (500 MHz, $CDCl_3$): δ (ppm) 8.88–8.86 (m, 4H), 8.84–8.82 (m, 4H), 8.51–8.49 (m, 2H), 8.14–8.10 (m, 2H), 8.05–8.01 (m, 2H), 8.00–7.97 (m, 4H), 7.42–7.37 (m, 2H), 7.11–7.07 (m, 4H), 4.12–4.09 (m, 4H), 3.76–3.74 (m, 4H), 3.55–3.53 (m, 4H), 3.48–3.47 (m, 8H), 3.43–3.41 (m, 4H), 3.38–3.37 (m, 4H), 3.29–3.27 (m, 4H), 3.11 (s, 6H); UPLC TOF MS ES+: $C_{62}H_{64}N_4O_{10}ZnI_2$ m/z=1341.8599, calcd. m/z=1342.2003; UV/vis (ACN : THF): λ_{max}=424 nm.

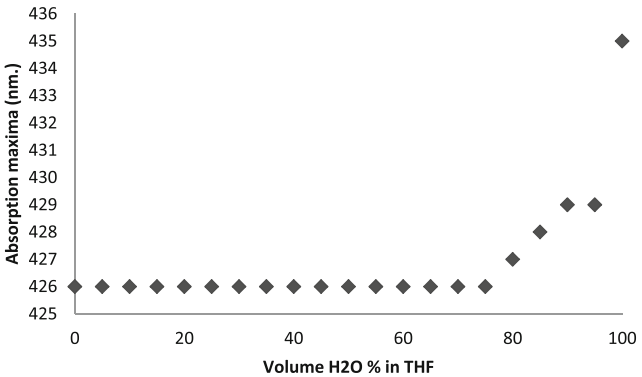

Fig. 8 Plot of absorption maxima of 10–6 M 5b vs the volume percent of water in THF. All the solutions prepared 5b content is 10–6 M

Preparation of Porphyrin Polymer 6a

The porphyrin monomer (5a), trimethylsilylacetylene were dissolved in a solvent mixture of THF and diisopropylamine in a 10 mL microwave tube. The mixture was degassed and purged with nitrogen. $Pd(PPh_3)_2Cl_2$ and CuI were added. The mixture was further carefully degassed. The sealed tube was heated and stirred at 60°C with 300 W maximum powers over

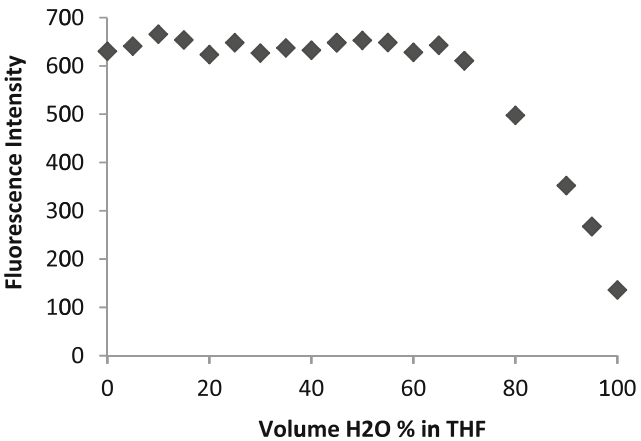

Fig. 10 Plot of fluorescence intensity of 10–6 M 5b vs the volume percent of water in THF. All the solutions prepared 5b content is 10–6 M

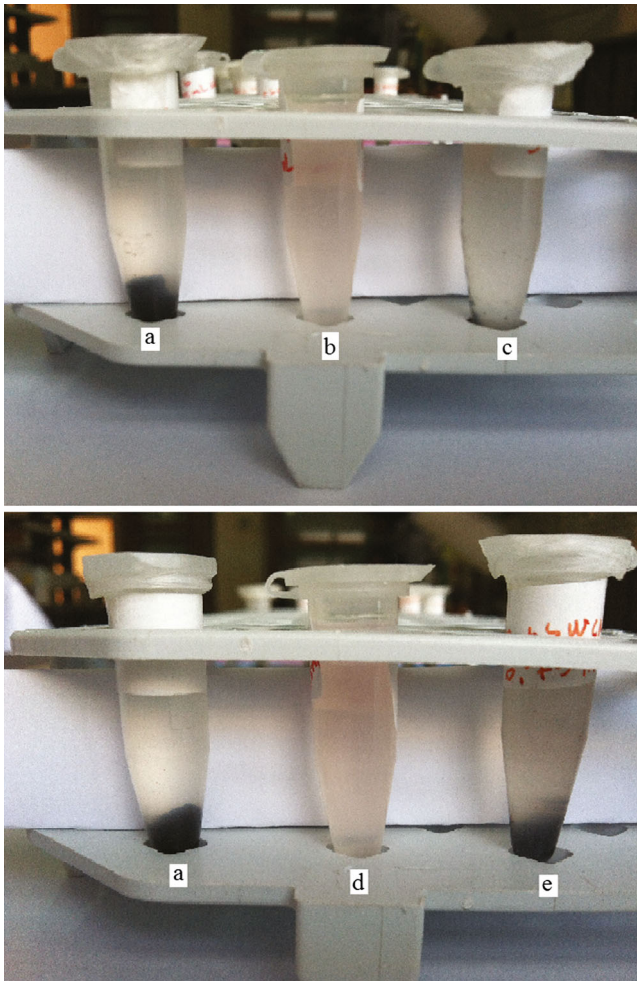

Fig. 11 Photographs of THF solutions of **a**) SWCNT, **b**) 5a, **c**) an equimolar mixture of 5a and SWCNT, **d**) 5b, and **e**) an equimolar mixture of 5b and SWCNT. All the photographs were taken after the ultrasonication and centifugation (10,000 rpm) steps

8 h under super cooling conditions. Then more THF was added in to the reaction mixture and washed with saturated ammonium chloride and brine solutions. The organic phase was dried with $MgSO_4$, and the solvent removed under vacuum to afford 6a. GPC (THF): M_w=4200 g/mol, M_n=3800 g/mol, M_p=4300 g/mol, PDI (M_w / M_n)=1.1

Preparation of Porphyrin Polymer 6b

The porphyrin monomer (5b), trimethylsilylacetylene were dissolved in a solvent mixture of THF and diisopropylamine in a 10 mL microwave tube. The mixture was degassed and purged with nitrogen. $Pd(PPh_3)_2Cl_2$ and CuI were added. The mixture was further carefully degassed. The sealed tube was heated and stirred at 60°C with 300 W maximum powers over 8 h under super cooling conditions. Then more THF was added in to the reaction mixture and washed with saturated ammonium chloride and brine solutions. The organic phase was dried with $MgSO_4$, and the solvent removed under vacuum to afford 6b. GPC (THF): M_w=5300 g/mol, M_n=3200 g/mol, M_p=6000 g/mol, PDI (M_w / M_n)=1.6

Results and Discussion

Spectroscopic Results

5a and 5b monomers and 6a and 6b oligomers have a well shaped absorption maximum at 426 nm in THF (Table 1, Figs. 1, 6, 12, and 15). The absorption maxima for both monomers were 10 and 9 nm red shifted in water, respectively for 5a and 5b and there were decreases in absorption intensities in comparison to the absorption in THF. Both monomers and oligomers synthesised had two intense emission bands at 605 and 654 nm, 604 and 654 nm, 604 and 653 nm, 615 and 652 nm in THF for 5a, 5b, 6a and 6b respectively. (Table 1, Figs. 4, 9, 13, and 16). Both of the emission bands of 5a and 5b were also red shifted to 609 and 659 nm, and 606 and 656 nm for 5a and 5b respectively, in water in comparison

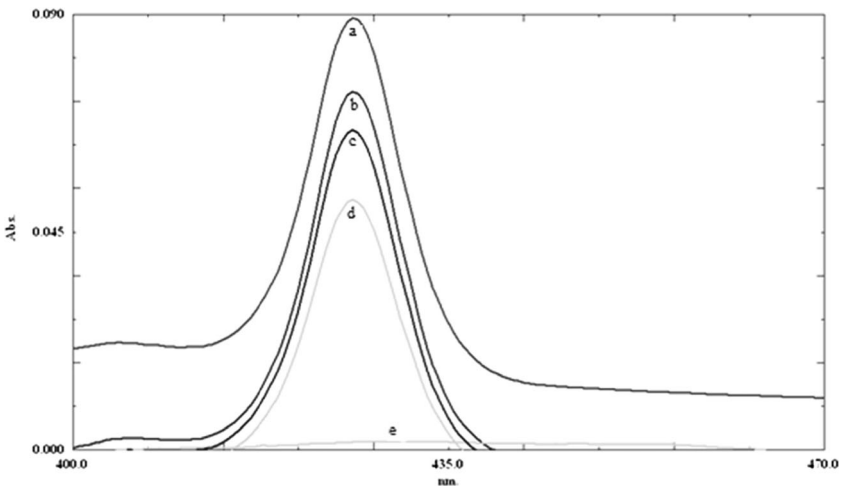

Fig. 12 UV/Vis spectra of **a**) 5b (0.005 mg 5b / 10 mL THF), **b**) 5b and SWCNT (0.005 mg 5b and 0.005 mg SWCNT / 10 mL THF), **c**) 5a (0.005 mg 5a / 10 mL THF), **d**) 5a and SWCNT (0.005 mg 5a and 0.005 mg SWCNT / 10 mL THF), and **e**) SWCNT (0.005 mg SWCNT / 10 mL THF) in THF after ultrasonication and centrifugation

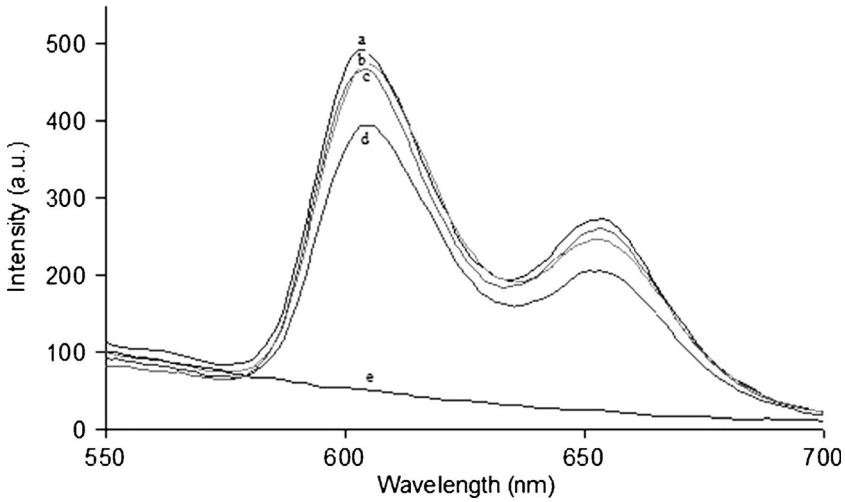

Fig. 13 Emission spectra of **a**) 5b (0.005 mg 5b / 10 mL THF), **b**) 5a (0.005 mg 5a / 10 mL THF), **c**) 5b and SWCNT (0.005 mg 5b and 0.005 mg SWCNT / 10 mL THF), **d**) 5a and SWCNT (0.005 mg 5a and 0.005 mg SWCNT / 10 mL THF), and **e**) SWCNT (0.005 mg SWCNT / 10 mL THF) in THF after ultrasonication and centrifugation

to THF and also quenching occurred. While this red shift for 5a was 4 nm, for 5b it was 2 nm. The shifts observed in the absorption and emission maxima of 5a and 5b in water were presumably due to the increase of the polarity of the environment of the monomers in water in comparison to the data obtained in THF. While the absorption maxima of 6a and 6b oligomers are the same, their emission maxima were different. While the first band of 6a appeared at 604 nm, the one for 6b was observed at longer wavelength as 615 nm. 6b exhibited significantly red-shifted emission maxima relative to the corresponding monomer.

Titration Experiment

Titrations of porphyrin derivatives 5a and 5b were performed at fixed concentration of 10^{-6} M 5a and 5b at different volume percent of water in THF by using an excitation wavelength of 426 nm (Figs. 1, 2, 3, 4, 5, 6, 7, 8, 9 and 10). The titration was monitored by following the absorbance and fluorescence changes on 5a and 5b spectra. As the water percent is increased the absorption and emission intensities decreased of both porphyrins 5a and 5b. For 5a, when increasing the water percent from 75 to 80 % a dramatic decrease in absorption intensity was observed (Figs. 1 and 2). The absorption maxima of 5a is as 426 nm till the water percent is 80 % and at 85 % water is red shifted to 436 nm and at 85 % and to 437 nm and then till 100 % water content it is 437 nm (Fig. 3). The fluorescence intensity of 5a showed a dramatic decrease when water percent was increased from 75 to 85 % (Figs. 4 and 5). In comparison to the absorption maxima at emission maxima there was a slight red shift when increasing the water percent from 75 to 85 % from 605 to 607 nm and at 100 % water is shifted to 609 nm (Fig. 4). The absorption and emission decrease of 5b was different than 5a. While there was a slight decrease at absorption maxima till 75 % water for 5b, the absorption intensity decreased gradually after 75 % percent of water till 100 % (Figs. 6 and 7). The absorption maxima for 5b was as 426 nm till 75 % percent of water and at

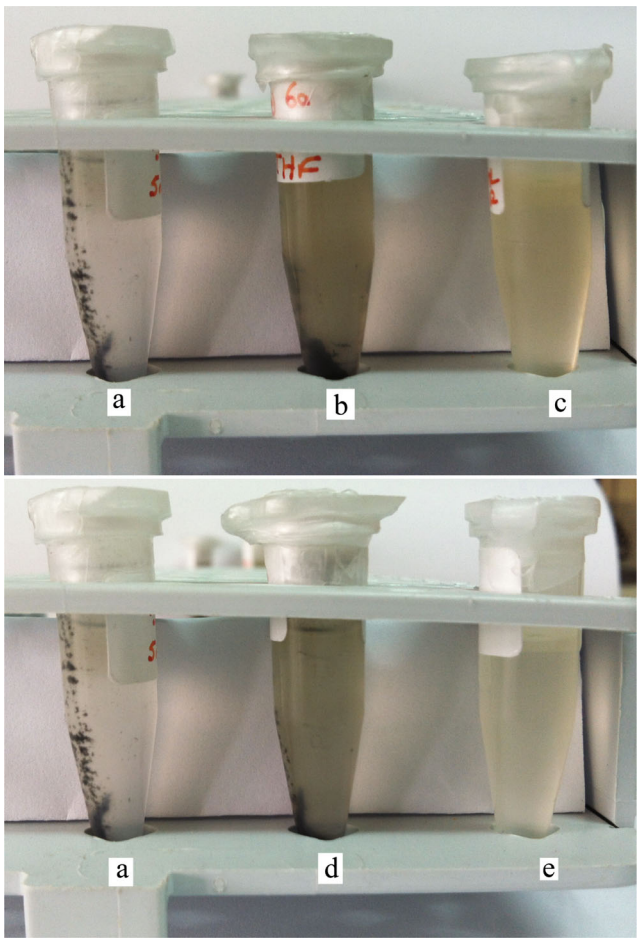

Fig. 14 Photographs of THF solutions of **a**) SWCNT (1 mg SWCNT / 5 mL THF), **b**) 6a and SWCNT (0.05 mg 6a and 1 mg SWCNT / 5 mL THF), **c**) 6a (0.05 mg 6a / mL THF), **d**) 6b and SWCNT (0.3 mg 6b and 1 mg SWCNT / 5 mL THF) and **e**) 6b (0.3 mg 6b / 5 mL THF). All the photographs were taken after the ultrasonication and centifugation (10,000 rpm) steps

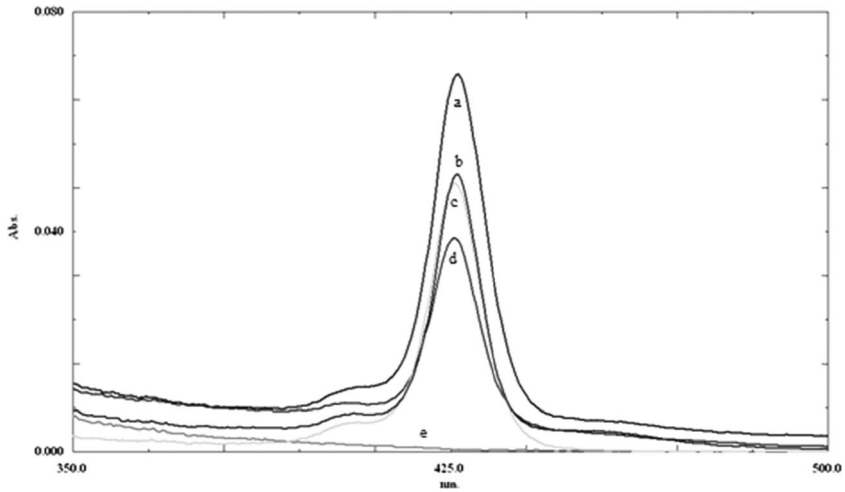

Fig. 15 UV/Vis spectra of **a**) 6a (0.001 mg 6a / 5 mL THF), **b**) 6a and SWCNT (0.001 mg 6a and 0.02 mg SWCNT / 5 mL THF), **c**) 6b (0.006 mg 6b / 5 mL THF), **d**) 6b and SWCNT (0.006 mg 6b and 0.02 mg SWCNT / 5 mL THF), and **e**) SWCNT (0.02 mg SWCNT / 5 mL THF) in THF after ultrasonication and centrifugation

80 % was as 427 nm, at 85 % as 428 nm, at 90–95 % as 429 nm and at 100 % shifted to 435 nm (Figs. 6 and Fig. 8). There was a slight decrease at fluorescence intensity of 5b till 70 % percent of water and after 70 % percent the fluorescence intensity decreased gradually (Figs. 9 and 10). Up to 80 % of water the emission maxima of 5b was 604 nm, and at % 85 there was a slight red shift to 605 nm. While for 5a the emission maxima shift was 5 nm as increasing the water content, for 5b only 1 nm shift was observed. In highly aqueous solvent mixtures, the changes in optical properties of the monomers are presumably due to hydrogen-bonding of the porphyrin derivatives with water. The broadening of the absorption band as the water percent of the solvent (85–100 % water) is increased was observed which may be originated from charge transfer transitions.

Mixing of the Porpyrin Derivatives with SWCNT

The solution behaviour of 5a, 5b, 6a, 6b and their equimolar mixture before and after solubilisation of SWCNT's in THF solutions was monitored both by visual inspection with the naked eye and more precisely using UV–vis and fluorescence spectroscopy (Figs. 11, 12, 13, 14, 15 and 16). SWCNT samples were ultrasonicated in the presence of porphyrins 5a, 5b and their oligomers 6a, 6b and then centrifugated. Binding of 5a, 5b, 6a, 6b onto surfaces of SWCNTs was investigated by absorption and emission spectroscopy. There was a decrease at absorption intensities of 5a, 5b, 6a, 6b and also fluorescence intensities were quenched after treatment with SWCNTs indicating solubilisation of SWCNTs. The decrease in absorption and emission spectra of oligomers were more than the decrease observed for monomers, indicating that oligomers solubilisation of SWCNTs is better than monomers. Clearly, porphyrin oligomers, 6a and 6b exhibits stronger binding interactions than monomers 5a and 5b, due to the extended π conjugation and enhanced electron donating character. Solubilisation probably occurs through the stepwise interactions that operate when the flat π surfaces of metalloporphyrins are rapidly adsorbed onto the curved π surfaces of SWCNT bundles. Porpyrins have an affinity to bind noncovalently with SWCNTs. The noncovalent bonding interaction of the SWCNTs is a desired property because of providing a further opportunity to employ these entitities as chemical and/or biological sensors. The SWCNTs can provide an ideal network to promote charge transfer in porphyrin-based systems and transport electrons to the collecting surface.

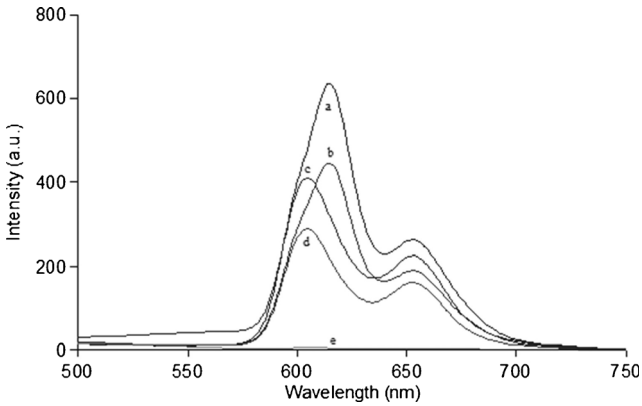

Fig. 16 Emission spectra of **a**) 6b (0.006 mg 6b / 5 mL THF), **b**) 6b and SWCNT (0.006 mg 6b and 0.02 mg SWCNT / 5 mL THF), **c**) 6a (0.001 mg 6a / 5 mL THF) **d**) 6a and SWCNT (0.001 mg 6a and 0.02 mg SWCNT / 5 mL THF) and **e**) SWCNT (0.02 mg SWCNT / 5 mL THF) in THF after ultrasonication and centrifugation

Conclusion

Porpyrin monomers 5a and 5b and their oligomers 6a and 6b were synthesised for the first time. Spectroscopic properties of 5a and 5b porphyrin monomers have common features. The titration experiment for the porphyrin monomers 5a and 5b were carried out in THF with different percentages of water. As the water percent is increased the absorption and emission intensities of both porphyrins 5a and 5b decreased. The newly

prepared porphyrin constructs were mixed with SWCNTs and data obtained indicates that oligomers, 6a and 6b, dissolve SWCNs better than monomers 5a and 5b, which make them candidates to generate noncovalent hybrid materials. The noncovalent nanotube functionalization with porphyrins is based on π – π – interactions between the porphyrin and SWCNT and thus does not disrupt the intrinsic electronic structure of SWCNTs, which is important for electronic applications.

Acknowledgments This work was supported by DGF (German Research Foundation) and TÜBİTAK (The Scientific and Technological Research Council of Turkey). I would like to express my gratitude to Prof. Dr. Stefan Hecht for giving opportunity to work in his lab and sharing all his ideas throughout the whole study. I also would like to thank to Dr. Zhilin Yu for his help during the experiments.

References

1. Götz DCG, Bruhn T, Senge MO, Bringmann G (2009) Synthesis and stereochemistry of highly unsymmetric β-meso-linked porphyrin arrays. J Org Chem 74:8005–8020
2. Calvete M, Yang GY, Hanack M (2004) Porphyrins and phthalocyanines as materials for optical limiting. Synth Met 141:231–243
3. Peters MV, Goddard R, Hecht S (2006) Synthesis and characterization of azobenzene-confined porphyrins. J Org Chem 71:7846–7849
4. Starners SD, Rudkevich DM, Rebek J (2001) Cavitands – porphyrins. J Am Chem Soc 123:4659–4669
5. Hecht S, Ihre H, Frechet MJ (1999) Porphyrin core star polymers: synthesis, modification and implication for site isolation. J Am Chem Soc 121:9239–9240
6. Matos MS, Hofkens J, Verheijen W, De Schryver FC, Hecht S, Pollak KW, Frechet JMJ, Forier B, Dehaen W (2000) Effect of core structure on photophysical and hydrodynamic properties of porphyrin dendrimers. Macromolecules 33:2967–2973
7. Hecht S, Emrick T, Frechet MJ (2000) Hyperbranched porphyrins- a rapid synthetic approach to multiporphyrin macromolecules. Chem Commun 313–314
8. Li WS, Aida T (2009) Dendrimer porphyrins. Chem Rev 109:6047–6076
9. Duggan SA, Fallon G, Langford SJ, Lau VL, Satchell JF, Paddon-Row MN (2001) Crown-linked porphyrin systems. J Org Chem 66: 4419–4426
10. Sun D, Tham FS, Reed CA, Chaker L, Burgess M, Boyd PDW (2000) Porphyrin-fullerene host-guest chemistry. J Am Chem Soc 122:10704–10705
11. Jasat A, Dolphin D (1997) Expanded porphyrins and their heterologs. Chem Rev 97:2267–2340
12. Muresan AZ, Thamyongkit P, Diers JR, Holten D, Lindsey JS, Boican DF (2008) Regiospecifically α-^{13}C-labeled porphyrins for studies of ground-state hole transfer in multiporphyrin arrays. J Org Chem 73:6947–6959
13. Harth EM, Hecht S, Helms B, Malmstorm EE, Frechet JMJ, Hawker CJ (2002) The effect of macromolecular architecture in nanomaterials: a comparison of site isolation in porphyrin core dendrimers and their isomeric linear analogues. J Am Chem Soc 124:3926–3938
14. Hecht DS, Ramirez RJA, Briman M, Artukovic E, Chichak KS, Stoddart JF, Grüner G (2006) Bioinspired detection of light using a porphyrin-sensitized single-wall nanotube field effect transistor. Nano Lett 6:2031–2036
15. Tagmatarchis N, Prato M, Guldi DM (2005) Soluble carbon nanotube ensembles for light-induced electron transfer interactions. Phys E 29: 546–550
16. Schuster DI, MacMahoni S, Guldi DM, Echegoyen L, Braslavsky SE (2006) Synthesis and photophysics of porphyrin-fullerene donor-acceptor dyads with conformationally flexible linkers. Tetrahedron 62: 1928–1936
17. Santos J, Illescas BM, Wielopolski M, Silva AMG, Tome AC, Guldi DM, Martin N (2008) Efficient electron transfer in β-substituted porphyrin-C_{60} dyads connected through a p-phenylenevinylene dimer. Tetrahedron 64:11404–11408
18. Hauke F, Atalick S, Guldi DM, Hirsch A (2006) Covalently linked heterofullerene-porphyrin conjugates; new model systems for long-lived intramolecular charge separation. Tetrahedron 62:1923–1927
19. Ros TD, Prato M, Carano M, Ceroni P, Paolucci F, Roffia S, Valli L, Guldi DM (2000) Synthesis, electrochemistry, Langmuir-Blodgett deposition and photophysics of metal-coordinated fullerene-porphyrin dyads. J Organomet Chem 599:62–68
20. Schuster DI, Li K, Guldi DM (2006) Porphyrin-fullerene photosynthetic model systems with rotaxane and catenane architectures. Comptes Rendus Chimie 9:892–908
21. Chichak KS, Star A, Altoe MVP, Stoddart JF (2005) Single-walled carbon nanotubes under dynamic coordination and supramolecular chemistry. Small 1:452–461
22. Zhao YL, Stoddart JF (2009) Noncovalent functionalization of single-walled carbon nanotubes. Acc Chem Res 42:1161–1171
23. Zhao YL, Hu L, Grüner G, Stoddart JF (2008) A tunable photosensor. J Am Chem Soc 130:16996–17003
24. Guldi DM, Rahman GMA, Jux N, Balbinot D, Hartnagel U, Tagmatarchis N, Prato M (2005) Functional single-wall carbon nanotube nanohybridss associating SWNTs with water-soluble enzyme model systems. J Am Chem Soc 127:9830–9838
25. Ehli C, Rahman GMA, Jux N, Balbinot D, Guldi DM, Paolucci F, Marcaccio M, Paolucci D, Melle-Franco M, Zerbetto F, Campidelli S, Prato M (2006) Interactions in single wall carbon nanotubes/pyrene/porphyrin nanohybrids. J Am Chem Soc 128:11222–11231
26. Huang CZ, Liao QG, Li YF (2008) Non-covalent anionic porphyrin functionalized multi-walled carbon nanotubes as an optical probe for specific DNA detection. Talanta 75:163–166
27. Dembinska B, Kulezsa PJ (2009) Multi-walled carbon nanotube-supported tungsten oxide-containing multifunctional hybrid electrocatalytic system for oxygen reduction in acid medium. Electrochim Acta 54:4682–4687
28. Luz RCS, Damos FS, Tanaka AA, Kubota LT, Gushikem Y (2008) Electrocatalysis of reduced L-glutathione oxidation by iron (III) tetra-(n-methyl-4-pyridyl)-porphyrin (FeT4MPyP) adsorbed on multi-walled carbon nanotubes. Talanta 76:1097–1104
29. Okunola A, Kowalewska B, Bron M, Kulezsa PJ, Schuhmann W (2009) Electroanalytic reduction of oxygen at electropolymerized films of metalloporphyrins deposited onto multi-walled carbon nanotubes. Electrochim Acta 54:1954–1960
30. Hyland MA, Morton MD, Brückner C (2012) Meso-tetrakis(pentafluorophenyl)porphyrin-derived chromene-annulated chlorins. J Org Chem 77:3038–3048
31. Cao X, Lin W, Yu Q (2011) A ratiometric fluorescent probe for thiols based on a tetrakis(4-hydroxyphenyl)porphyrin–coumarin scaffold. J Org Chem 76:7423–7430
32. Carofiglio T, Varotto A, Tonellato U (2004) One-Pot synthesis of cyanuric acid-bridged porphyrin−porphyrin dyads. J Org Chem 69: 8121–8124
33. Ho KHL, Rivier L, Jousselme B, Jegou P, Filoramo A, Campidelli S (2010) Zn-porphyrin/Zn-phthalocyanine dendron for SWNT functionalisation. Chem Comm 46:8731–8733
34. Cheng F, Zhang S, Adronov A, Echegoyen L, Diederich F (2006) Triply fused Zn^{II}–porphyrin oligomers: synthesis, properties, and

supramolecular interactions with Single-Walled Carbon Nanotubes (SWNTs). Chem Eur J 12:6062–6070
35. Hasobe T, Fukuzumi S, Kamat PV (2005) Ordered assembly of protonated porphyrin driven by single wall carbon nanotubes. J- and H-aggregates to nanorods. J Am Chem Soc 127:11884–11885
36. Saito K, Troiani V, Qiu H, Solladie N, Sakata T, Mori H, Ohama M, Fukuzumi S (2007) Nondestructive formation of supramolecular nanohybrids of single-walled carbon nanotubes with flexible porphyrinic polypeptides. J Phys Chem C 111:1194–1199
37. Sprafke JK, Stranks SD, Warner JH, Nicholasa RJ, Anderson HL (2011) Noncovalent binding of carbon nanotubes by porphyrin oligomers. Angew Chem Int Ed 50:2313–2316
38. Stranks SD, Sprafke JK, Anderson HL, Nicholas RJ (2011) Electronic and mechanical modification of single-walled carbon nanotubes by binding to porphyrin oligomers. ACS NANO 5: 2307–2315
39. Zheng JY, Tashiro K, Hirabayashi Y, Kinbara K, Saigo K, Aida T, Sakamoto S, Yamaguchi K (2001) Cyclic dimers of metalloporphyrins as tunable hosts for fullerenes: a remarkable effect of rhodium(III). Angew Chem Int Ed 40:1857–1861
40. Balaz M, Colins HA, Dahlstedt E, Anderson HL (2009) Synthesis of hydrophilic conjugated porphyrin dimers for one-photon and two-photon photodynamic therapy at NIR wavelengths. Org Biomol Chem 7:874–888
41. Gil-Ramirez G, Karlen SD, Shundo A, Porfyrakis K, Ito Y, Briggs GAD, Morton JJL (2010) A cyclic porphyrin trimer as a receptor for fullerenes. Org Lett 12:3544–3547
42. Ravikanth M, Strachan JP, Li F, Lindsey JS (1998) Trans-Substituted porphyrin building blocks bearing iodo and ethynyl groups for applications in bioorganic and materials chemistry. Tetrahedron 54:7721–7734
43. Bonifazi D, Accorsi G, Armaroli N, Song F, Palkar A, Echegoyen L, Scholl M, Seiler P, Jaun B, Diederich F (2005) Oligoporphyrin arrays conjugated to [60] fullerene: preparation, NMR analysis, and photophysical and electrochemical properties. Helvetica Chimica Acta 88:1839–1884
44. Yamada H, Okujima T, Ono N (2008) N Supramolecules based on porphyrins. Top Heterocycl Chem 17:123–159
45. Ohira S, Bredas JL (2009) Porphyrin dimers: a theoretical understanding of the impact of electronic coupling strength on the two-photon absorption properties. J Mater Chem 19:7545–7550
46. Clausen C, Gryko DT, Dabke RB, Dontha N, Bocian DF, Kuhr WG, Lindsey JS (2000) Synthesis of thiol-derivatized porphyrin dimers and trimers for studies of architectural effects on multibit information storage. J Org Chem 65:7363–7370
47. Gentilini C, Boccalon M, Pasguato L (2008) Straightforward synthesis of fluorinated amphiphilic thiols. Eur J Org Chem 19:3308–3313
48. Kueny-Stotz M, Mamlouk-Chaouachi H, Felder-Flesch D (2011) Synthesis of patent blue derivatized hydrophilic dendrons dedicated to sentinel node detection in breast cancer. Tetrahedron Lett 52:2906–2909
49. Brunner H, Gruber N (2004) Carboplatin-containing porphyrin–platinum complexes as cytotoxic and phototoxic antitumor agents. Inorg Chim Acta 357:4423–4451